

Confined-Plume Chemical Deposition: Rapid Synthesis of Crystalline Coatings of Known Hard or Superhard Materials on Inorganic or Organic Supports by Resonant IR Decomposition of Molecular Precursors

Borislav L. Ivanov,[†] Matthew S. Wellons,^{‡,§} and Charles M. Lukehart^{*,‡}

Departments of Physics and Astronomy and Chemistry, Vanderbilt University, Nashville, Tennessee 37235

Received March 7, 2009; E-mail: chuck.lukehart@vanderbilt.edu

Abstract: A one-step process for preparing microcrystalline coatings of known superhard, very hard, or ultraincompressible ceramic compositions on either inorganic or organic supports is reported. Midinfrared pulsed-laser irradiation of preceramic chemical precursors layered between IR-transmissive hard/soft supports under temporal and spatial confinement at a laser wavelength resonant with a precursor vibrational band gives one-step deposition of *crystalline* ceramic coatings without incurring noticeable collateral thermal damage to the support material. Reaction plume formation at the precursor/laser beam interface initiates confined-plume, chemical deposition (CPCD) of crystalline ceramic product. Continuous ceramic coatings are produced by rastering the laser beam over a sample specimen. CPCD processing of the Re–B single-source precursor, $(B_3H_8)Re(CO)_4$, the dual-source mixtures, $Ru_3(CO)_{12}/B_{10}H_{14}$ or $W(CO)_6/B_{10}H_{14}$, and the boron/carbon single-source precursor, $\alpha-B_{10}C_2H_{12}$, confined between Si wafer or NaCl plates gives microcrystalline deposits of ReB_2 , RuB_2 , WB_4 , or B_4C , respectively. CPCD processing of Kevlar fabric wetted by $(B_3H_8)Re(CO)_4$ produces an oriented, microcrystalline coating of ReB_2 on the Kevlar fabric without incurring noticeable thermal damage of the polymer support. Similarly, microcrystalline coatings of ReB_2 can be formed on IR-transmissive IR2, Teflon, or Ultralene polymer films.

Introduction

As recently pointed out by Kaner et al., the quest for new superhard materials is driven by both scientific interest and practical objectives.¹ Diamond, the hardest known material, and cubic boron nitride, the second hardest known material, have deficiencies. Diamond is inefficient at cutting ferrous metals because of iron carbide formation, and cubic BN is formed on industrial scale only at high temperatures (>1500 °C) and pressures (>5 GPa), making it expensive. Superhard materials, defined as having hardness values greater than 40 GPa, must resist inelastic (or plastic) deformation by preventing irreversible, relative atomic motion.² High resistance to plastic deformation is favored by strong covalent bonding and can be introduced into heavy-metal materials by combining heavy metals with light elements (such as B, C, N, or O) in a 3D network of strong covalent bonding.

Computational studies have predicted that several second- or third-row transition-metal boride compositions should be ultraincompressible or very hard materials,^{2–6} and that several

new boron-rich compositions should be superhard materials.⁷ Consistent with these predictions, the ultraincompressibility of OsB_2 and superhardness of ReB_2 have been confirmed recently.^{8,9}

Microcrystalline ReB_2 is usually prepared at high temperatures ($T \geq 1000$ °C) by direct reaction of the elements.¹⁰ It is stable in dry air up to 500 °C, has a bulk modulus of 360 GPa and an average hardness of 48 GPa (for a grain size of ca. 10–15 μm), and can scratch the (100) plane of natural diamond. ReB_2 can be grown as single crystals at high temperature using floating-zone or aluminum-flux methods^{11–13} or deposited as a thin-film by pulsed-laser deposition onto a hot substrate (570 °C) under high vacuum at very low deposition rates.¹⁴ A wide variety of metal boride compositions have been prepared using

[†] Department of Physics and Astronomy.

[‡] Department of Chemistry.

[§] Present address: Savannah River National Laboratory, 999-2W, Savannah River Site, Aiken, SC 29808.

(1) Kaner, R. B.; Gilman, J. J.; Tolbert, S. H. *Science* **2005**, *308*, 1268.
 (2) Gou, H.; Hou, L.; Zhang, J.; Li, H.; Sun, G.; Gao, F. *Appl. Phys. Lett.* **2006**, *88*, 221904.
 (3) Wang, Y. X. *Appl. Phys. Lett.* **2007**, *91*, 101904.
 (4) Hao, X.; Xu, Y.; Wu, Z.; Zhou, D.; Liu, X.; Cao, X.; Meng, J. *Phys. Rev. B* **2006**, *74*, 224112.

(5) Hebbache, M.; Stuparevic, L.; Zivkovic, D. *Solid State Commun.* **2006**, *139*, 227.
 (6) Chiodo, S.; Gotsis, H. J.; Russo, N.; Sicilia, E. *Chem. Phys. Lett.* **2006**, *425*, 311.
 (7) Gao, F.; Qin, X.; Wang, L.; He, Y.; Sun, G.; Hou, L.; Wang, W. *J. Phys. Chem. B* **2005**, *109*, 14892.
 (8) Cumberland, R. W.; Weinberger, M. B.; Gilman, J. J.; Clark, S. M.; Tolbert, S. H.; Kaner, R. B. *J. Am. Chem. Soc.* **2005**, *127*, 7264.
 (9) Chung, H. Y.; Weinberger, M. B.; Levine, J. B.; Cumberland, R. W.; Kavner, A.; Yang, J. M.; Tolbert, S. H.; Kaner, R. B. *Science* **2007**, *316*, 436.
 (10) Placa, S. L.; Post, B. *Acta Crystallogr.* **1962**, *15*, 97.
 (11) Otani, S.; Aizawa, T.; Ishizawa, Y. *J. Alloys Compd.* **1997**, *252*, L19.
 (12) Otani, S.; Aizawa, T.; Ishizawa, Y. Japanese Patent JP10251095, 1998.
 (13) Levine, J. B.; Nguyen, S. L.; Rasool, H. I.; Wright, J. A.; Brown, S. E.; Kaner, R. B. *J. Am. Chem. Soc.* **2008**, *130*, 16953.
 (14) Latini, A.; Rau, J. V.; Ferro, D.; Teghil, R.; Albertini, V. R.; Barinov, S. M. *Chem. Mater.* **2008**, *20*, 4507.

chemical vapor deposition (CVD) synthesis strategies,^{15–24} although formation of *crystalline* metal borides by CVD usually requires depositing material on heated surfaces ($T \geq 500$ °C) or by postdeposition thermal annealing of amorphous material at high temperatures.

Experimental verification of the superhardness of ReB_2 and the availability of potential single-source molecular precursors containing rhenium and boron inspired a search for new chemical synthesis strategies to synthesize crystalline ReB_2 (or other hard materials compositions) utilizing preceramic precursors. Developing a method by which known crystalline, hard, or superhard materials could be formed as coatings on either hard *or* soft substrates to enhance surface properties might also have practical importance. We now report the fortuitous discovery of a confined-plume chemical deposition (CPCD) synthesis strategy for the preparation of microcrystalline coatings of ReB_2 on either hard *or* soft supports using resonant infrared (IR) decomposition of appropriate molecular precursors. CPCD syntheses were performed under near-ambient laboratory-frame conditions of temperature and pressure without requiring special high-temperature or high-pressure equipment and were extended in scope to include the preparation of other known hard or superhard crystalline ceramics (RuB_2 , WB_4 , or B_4C).

Results and Discussion

CPCD Synthesis of Microcrystalline Coatings of Known Hard or Superhard Materials on Inorganic Supports by Resonant IR Degradation of Molecular Precursors. Given the availability of a tunable, IR free-electron laser (FEL) facility at Vanderbilt University and a potential single-source molecular precursor, $(\text{B}_3\text{H}_8)\text{Re}(\text{CO})_4$, **1**,^{25,26} for the known superhard material, ReB_2 , the possibility of preparing hexagonal ReB_2 from molecular precursor **1** using resonant FEL IR radiation to initiate precursor decomposition was investigated.

Complex **1**, $(\text{B}_3\text{H}_8)\text{Re}(\text{CO})_4$, is an ideal molecular precursor to ReB_2 in three respects: (1) It is stable to air oxidation on the time scale of several hours, which is convenient when working in the open atmosphere; (2) it is a viscous liquid at room temperature allowing for easy application onto substrate surfaces; and (3) it has a boron-rich composition (1:3 Re/B stoichiometry) which mitigates against loss of boron during synthesis. Since ReB_2 is the phase of highest boron content in the Re–B phase diagram,²⁷ bulk syntheses of ReB_2 usually require an excess of boron to ensure complete formation of ReB_2 . (Bulk synthesis of ReB_2 in sealed tubes is successful when

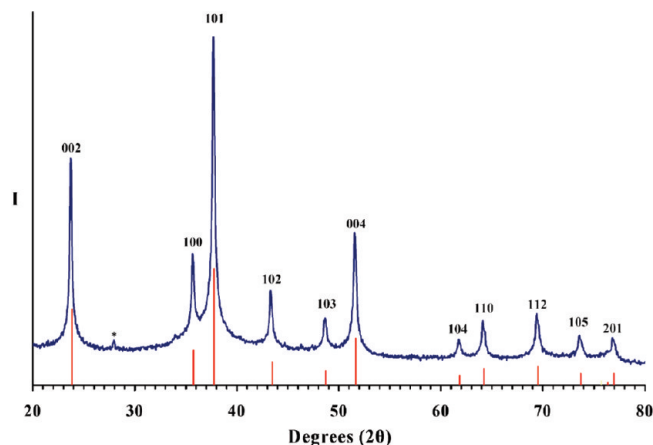


Figure 1. XRD scan of as-prepared ReB_2 formed on a Si(510) zero-background wafer by irradiation of a Si wafer/precursor **1**/Si wafer layered sample specimen with resonant FEL IR radiation. The XRD line pattern shown in red is that of ReB_2 (PDF #11-581). The peak at ca. 28° in 2θ (*) is assigned to B_2O_3 .

using stoichiometric amounts of Re and B powders, as boron loss is precluded under such conditions.⁹)

Resonant, pulsed FEL IR radiation, tuned to the most intense $\text{C}\equiv\text{O}$ or $\text{B}-\text{H}$ stretching vibrations of precursor **1**, was rastered over sample specimens consisting of precursor **1** confined between two layers of solid support in an open, ambient-atmosphere setting. Initially, hard supports, such as Si wafers (p-type Si(100) or Si(510) wafers) or NaCl plates, were used as sample supports, since both materials are highly transparent to FEL IR radiation (Supporting Information).

Initial experimental results proved disappointing. When complex **1** was applied to the unpolished surface of a $1\text{ cm} \times 1\text{ cm}$ Si wafer by filling surface voids (ca. 0.005 mm depth) and then scanned with resonant FEL IR radiation (either 5.1 or $3.9\text{ }\mu\text{m}$) in open air or under N_2 gas with either top-side or bottom-side illumination, precursor decomposition was evidenced by plume formation at the point of irradiation. However, product identification, determined solely by powder X-ray diffraction (XRD), revealed only Re metal, ReSi_2 , ReO_3 , or unidentified amorphous material as products. ReB_2 formation could not be confirmed.

These results indicate that separation of Re and B atoms occurs probably because of either predominant vaporization or reaction of vapor species with atmospheric gases. To inhibit both possibilities, a thin film of precursor **1** was *confined* between two Si wafers and then scanned with resonant FEL IR light at either 5.1 or $3.9\text{ }\mu\text{m}$. A black, reflective powder formed between the Si wafers and XRD scans (Figure 1) indicate formation of ReB_2 as the only crystalline product (along with a small amount of B_2O_3). Scanning electron microscope (SEM) and high-resolution transmission electron microscope (HRTEM) images (Figure 2) of this product reveal deposition of hexagonal platelets of ReB_2 . These platelets are arranged in parallel linear strips along the rastering direction with hexagonal facets oriented nearly perpendicular to the substrate surface. Lattice fringes are observed showing lattice spacings having measured d -spacings of 2.38 and $3.76\text{ }\text{\AA}$, consistent with d -spacings of 2.38 and $3.74\text{ }\text{\AA}$ known for the (101) and (002) lattice planes of hexagonal ReB_2 , respectively.¹⁰ In control experiments, heating Si wafer/precursor **1**/Si wafer specimens in a tube furnace or by rapid microwave irradiation gives only Re metal with no detectable formation of ReB_2 or any other rhenium boride composition as

- (15) Chen, C.; Wang, X.; Lu, Y.; Jia, Z.; Guo, J.; Wang, X.; Zhu, M.; Xu, X.; Xu, J.; Feng, Q. *Physica C* **2004**, *416*, 90.
- (16) Zhang, H.; Zhang, Q.; Tang, J.; Qin, L.-C. *J. Am. Chem. Soc.* **2005**, *127*, 2862.
- (17) Kher, S. S.; Spencer, J. T. *J. Phys. Chem. Solids* **1998**, *59*, 1343.
- (18) Amini, M. M.; Fehner, T. P.; Long, G. J.; Politowski, M. *Chem. Mater.* **1990**, *2*, 432.
- (19) Jensen, J. A.; Gozum, J. E.; Pollina, D. M.; Girolami, G. S. *J. Am. Chem. Soc.* **1988**, *110*, 1643.
- (20) Yang, Y.; Jayaraman, S.; Kim, D. Y.; Girolami, G. S.; Abelson, J. R. *J. Cryst. Growth* **2006**, *294*, 389.
- (21) Yang, Y.; Jayaraman, S.; Kim, D. Y.; Girolami, G. S.; Abelson, J. R. *Chem. Mater.* **2006**, *18*, 5088.
- (22) Goedde, D. M.; Girolami, G. S. *J. Am. Chem. Soc.* **2004**, *126*, 12230.
- (23) Goedde, D. M.; Windler, G. K.; Girolami, G. S. *Inorg. Chem.* **2007**, *46*, 2814.
- (24) Kin, D. Y.; Yang, Y.; Abelson, J. R.; Girolami, G. S. *Inorg. Chem.* **2007**, *46*, 9060.
- (25) Gaines, D. F.; Hildebrandt, S. J. *J. Am. Chem. Soc.* **1974**, *96*, 5574.
- (26) Gaines, D. F.; Hildebrandt, S. J. *Inorg. Chem.* **1978**, *17*, 794.
- (27) *Binary Alloy Phase Diagrams*; Massalski, T. B., Ed.; ASM International: Materials Park, OH, 1990.

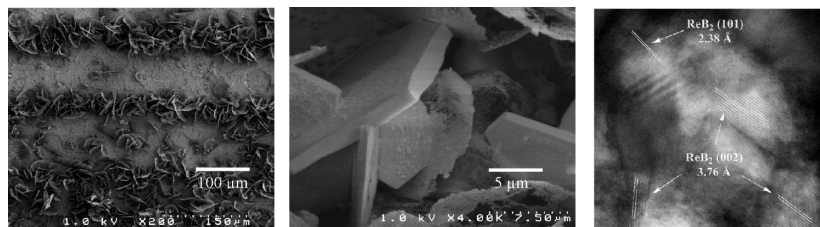


Figure 2. SEM images of ReB_2 microcrystal deposition on Si wafer support by CPCD processing showing linear strips at low magnification (left image) and partially oriented hexagonal platelets at higher magnification (middle image). HRTEM micrograph at 400 k magnification (right image) showing fringe patterns matching those known for hexagonal ReB_2 .

crystalline phases. A CPCD synthesis strategy using resonant laser excitation enables one-step decomposition of precursor 1 and growth of ReB_2 microcrystals.

Crystalline ceramic coatings having compositions other than ReB_2 can also be formed by CPCD using either single-source or dual-source chemical precursors. Resonant FEL IR irradiation of NaCl plate/precursor layer/Si(510) wafer layered assemblies (where the precursor layer contains (1) an intimate mixture of $\text{Ru}_3(\text{CO})_{12}$ and $\text{B}_{10}\text{H}_{14}$, (2) an intimate mixture of $\text{W}(\text{CO})_6$ and $\text{B}_{10}\text{H}_{14}$, or (3) solely $o\text{-B}_{10}\text{C}_2\text{H}_{12}$) at frequencies tuned to a vibrational frequency of a precursor IR absorption band ($5.1 \mu\text{m}$ for metal carbonyl precursors and $3.85 \mu\text{m}$ for $o\text{-B}_{10}\text{C}_2\text{H}_{12}$) forms microcrystalline deposits of ultrahard RuB_2 ,²⁸ superhard WB_4 ,²⁹ or hard B_4C ,³⁰ respectively, on Si wafer supports. Platelet deposition morphologies are evident from SEM micrographs of the RuB_2 (Figure 3A) and B_4C (Figure 3B) products, and all product compositions and purity levels have been confirmed by powder XRD (Figure 3C). ReB_2 microcrystalline coatings have also been prepared from mixtures of the *dual-source* precursors $\text{Re}_2(\text{CO})_{10}$ and $\text{B}_{10}\text{H}_{14}$ (see Supporting Information for an XRD scan). ReB_2 and WB_4 are known to possess sufficient hardness to scratch diamond.^{31,32} CPCD processing is the only *chemical* (i.e., molecular precursor-based) deposition method known for preparing crystalline thin films of these materials, though pulsed-laser deposition of ReB_2 has been reported.¹⁴

To obtain information about conditions present during CPCD processing, a preliminary energy analysis of CPCD laser-initiated reactions was performed. Using a beam splitter and two synchronized energy meters, we split the incident pulsed-laser FEL IR beam into two beams. One beam (ca. 5% of incident IR radiation) passes directly onto an energy meter, while the other beam (ca. 95% of incident IR radiation) passes through a confined NaCl plate/precursor/NaCl plate specimen onto a second energy meter as a transmitted beam. By measuring the ratio of the energy readings of these two meters with and without precursor present, the percentage of incident IR energy absorbed by the precursor layer for each pulse can be measured and calculated.

When the FEL beam is rastered, the incident IR beam encounters a continuous supply of precursor, and IR absorption occurs mostly by excitation of precursor vibrational bands with

some undetermined amount of IR absorption (or scattering) by any formed ceramic product. Plots of percent absorbed energy versus number of FEL IR macropulses are shown in Figure 4 when using either $(\text{B}_3\text{H}_8)\text{Re}(\text{CO})_4$ or $o\text{-B}_{10}\text{C}_2\text{H}_{12}$ as single-source precursor and a FEL beam scan rate of 1 mm/s. These data indicate that 75–95% of the incident FEL IR laser energy is absorbed by the CPCD process. An oscillation in such percent-absorbed energy plots reveals instabilities known to occur during laser-induced chemical processes.³³

If most of this absorbed energy initiates precursor decomposition on the pico- to microsecond time scale within a traveling spot path, it appears that any residual thermal energy readily dissipates from the CPCD reaction zone into a bulk specimen without causing noticeable collateral thermal damage. When the above experiment is performed using a *static* FEL beam (data not shown), only 10–15% energy absorption is observed following initial local precursor decomposition (presumably due to absorption by formed ceramic product), further indicating that complementary 85–90% of the incident energy absorption observed in the scanning experiment (discussed above) occurs by precursor decomposition.

Furthermore, when using a $350\text{-}\mu\text{m}$ laser spot diameter, an *o*-carborane precursor thickness of $40 \mu\text{m}$, a laser pulse energy of 21.5 mJ, and assuming no thermal energy losses to NaCl plates and temperature independence of all optical and thermal parameters, we calculate formation of a local temperature near 3000 K within the CPCD reaction plume during B_4C formation for a single laser macropulse (see Supporting Information for details). Using a reported model developed for laser-induced confined plasmas, we also estimate a local pressure of 2.04 GPa for a laser power density of $2.4 \text{ GW}/\text{cm}^2$ per 0.8 ps micropulse on the picosecond time scale (see Supporting Information for details).^{34,35} Under similar confinement conditions, laser-initiated plasma plume formation is known to occur at measured peak pressures between 0.6 and 5 GPa (when using laser power densities of $0.4\text{--}4 \text{ GW}/\text{cm}^2$).³⁶ While such local conditions would favor plasma formation during CPCD reactions, these conditions would exist only within microscale spatial confinement and on a pico- to microsecond time scale, thus permitting dissipation of any residual energy into the surrounding medium without causing substantial damage to a support material.

Various structure zone models have been developed to explain the morphological features of materials deposited

(28) Chung, H.-Y.; Weinberger, M. B.; Yang, J.-M.; Tolbert, S. H.; Kaner, R. B. *Appl. Phys. Lett.* **2008**, *92*, 261904.

(29) Bodorova, L. G.; Koval'chenko, M. S.; Serebryakova, T. I. *Powder Metall. Met. Ceram.* **1974**, *13*, 1.

(30) Werheit, H.; Leithe-Jaspar, A.; Tanaka, T.; Rotter, H. W.; Schwetz, K. A. *J. Solid State Chem.* **2004**, *177*, 575.

(31) Chung, H. Y.; Weinberger, M. B.; Levine, J. B.; Cumberland, R. W.; Kavner, A.; Yang, J. M.; Tolbert, S. H.; Kaner, R. B. *Science* **2007**, *318*, 1550.

(32) Gu, Q.; Krauss, G.; Steurer, W. *Adv. Mater.* **2008**, *20*, 1.

(33) Baeuerle, D. *Laser Processing and Chemistry*, 2nd ed.; Springer-Verlag: New York, 1996; pp 479–513.

(34) Fabbro, R.; Fournier, J.; Ballard, P.; Devaux, D.; Virmont, J. *J. Appl. Phys.* **1990**, *68*, 775.

(35) Peyre, P.; Fabbro, R. *Opt. Quantum Electron.* **1995**, *27*, 1213.

(36) Fairand, B. P.; Clauer, A. H. *J. Appl. Phys.* **1979**, *50*, 1497.

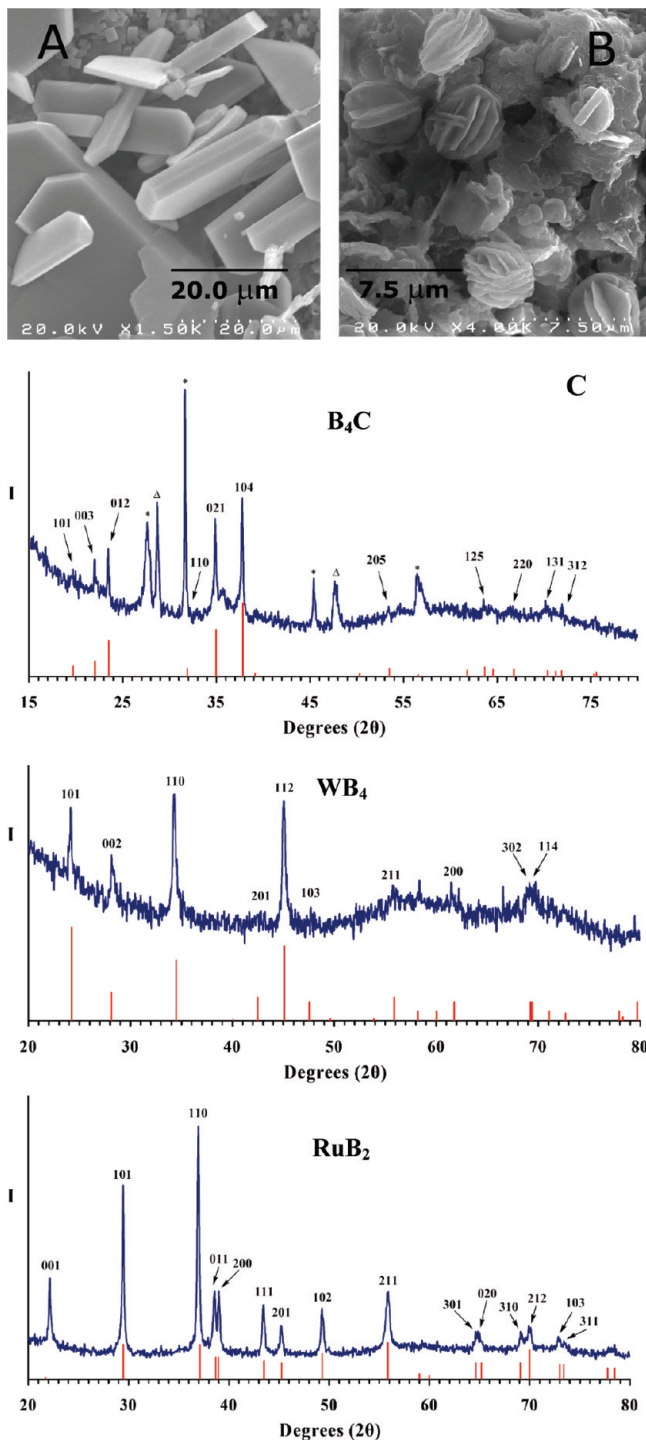


Figure 3. SEM images of RuB_2 platelets (A) and B_4C platelets (B) formed by resonant FEL IR irradiation of NaCl plate/precursor/Si wafer samples. XRD scans (C) of B_4C , WB_4 , and RuB_2 prepared by resonant FEL IR irradiation of NaCl plate/precursor/Si wafer sample specimens, where the precursors are a mixture of $\text{Ru}_3(\text{CO})_{12}$ and $\text{B}_{10}\text{H}_{14}$, a mixture of $\text{W}(\text{CO})_6$ and $\text{B}_{10}\text{H}_{14}$, and solely *o*- $\text{B}_{10}\text{C}_2\text{H}_{12}$, respectively. Standard XRD line patterns (red) of the corresponding pure bulk material [RuB_2 (PDF #15-0213); WB_4 (PDF #19-1373); B_4C (PDF #35-0798)]; * denotes diffraction from residual NaCl support; diffraction peaks denoted by Δ are from an unidentified substance.

under physical or chemical vapor deposition conditions as a function of temperature.^{37–40} Given the “zone 3” single-crystalline ReB_2 and B_4C microcrystalline morphologies (as defined within structure zone models) formed under resonant FEL IR laser CPCD processing conditions, a local temper-

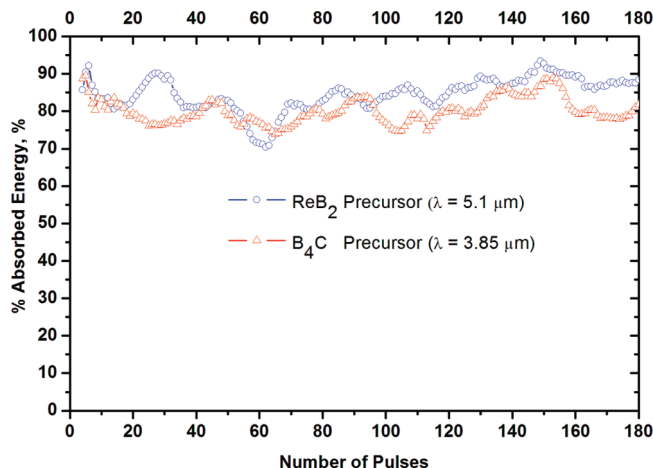


Figure 4. Plots of percent-absorbed energy versus number of laser macropulses for CPCD processing of NaCl plate/precursor/NaCl plate specimens when using the ReB_2 precursor, **1**, and the B_4C precursor, *o*- $\text{B}_{10}\text{C}_2\text{H}_{12}$, and a scanning FEL IR beam (1 mm/s) tuned to an IR adsorption band appropriate for each precursor.

ature between half of the melting temperature and the melting temperature of the ceramic product is predicted. The peak temperature estimated above for the B_4C CPCD reaction zone using laser energy density calculations (3000 K) is close to the known melting temperatures of ReB_2 (2673 K) and B_4C (2718 K), accordingly.

CPCD Synthesis of Microcrystalline Coatings of Known Very Hard or Superhard Materials on Organic Supports by Resonant IR Degradation of Molecular Precursors. If residual energy absorbed per pulse during CPCD processing dissipates throughout the bulk sample without causing significant bulk-material heating, then CPCD decomposition of precursors to form crystalline ceramic coatings might also occur on *soft material* supports, such as organic polymers, with only minimal thermal damage. Preliminary results described below confirm this prediction and demonstrate that IR-transmissive polymers, such as Kevlar fabric, IR2, Teflon, or Ultralene polymer films can serve as soft supports for CPCD synthesis of *crystalline* ReB_2 coatings using precursor **1**.

When commercial Kevlar fabric (1 cm × 1 cm specimen) wetted with the liquid chemical precursor (B_3H_8) $\text{Re}(\text{CO})_4$, **1**, and confined between two Si wafers is irradiated in ambient atmosphere laboratory-frame conditions with a pulsed FEL IR beam tuned to the most intense $\text{C}\equiv\text{O}$ stretching vibration of precursor **1** (5.1 μm), a vapor plume forms at the IR beam/precursor contact interface, indicating rapid decomposition of precursor molecules. By rastering the FEL beam across the sample in linear scans (1 mm/s) separated spatially by 150 μm , a 0.75 cm × 0.75 cm sample area can be reacted within 6 min.

Photographs and SEM micrographs reveal formation of hexagonal microplatelets of ReB_2 throughout the Kevlar fabric specimen as a black coating (Figure 5A–F). Both the top and bottom surfaces within the irradiated area of the Kevlar fabric specimen are blackened. Spatial confinement can also be provided by placing the wetted Kevlar fabric specimen between

(37) Fahrenholtz, W. G.; Hilmis, G. E.; Talmy, I. G.; Zaykoski, J. A. *J. Am. Ceram. Soc.* **2007**, *90*, 1347.

(38) Messier, R.; Giri, A. P.; Roy, R. A. *J. Vac. Sci. Technol.*, **1984**, *2*, 500.

(39) Monteiro, O. R. *Annu. Rev. Mater. Res.* **2001**, *31*, 111.

(40) Hlavacek, V.; Puszynski, J. A. *Ind. Eng. Chem. Res.* **1996**, *35*, 349.

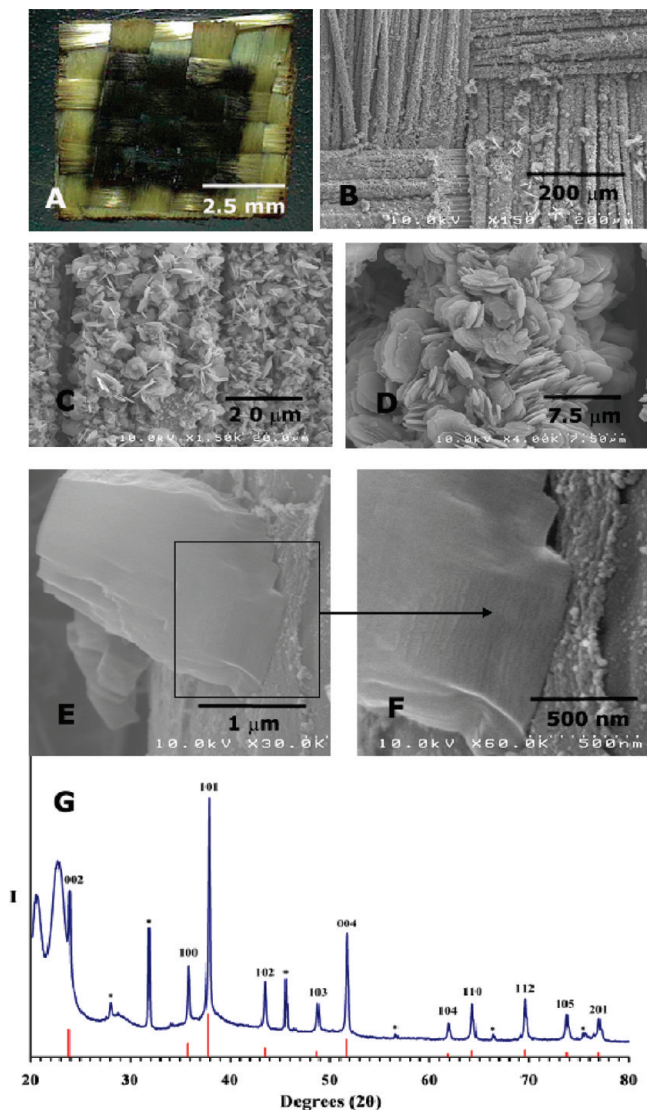


Figure 5. Photograph (A) and SEM images at three magnifications (B–D) of ReB_2 platelets formed on commercial Kevlar fabric using chemical precursor **1** and CPCD processing. SEM images at two magnifications showing the Kevlar fabric/ ReB_2 platelet interface (E, F). XRD scans (G) of ReB_2 hexagonal plates formed on commercial Kevlar fabric using chemical precursor **1**, confinement between two NaCl plates, and CPCD processing. Standard XRD line pattern (red) of bulk ReB_2 ; * denotes diffraction from residual NaCl support material; broad diffraction peaks at ca. 21° , 22° , and 29° in 2θ are known diffraction peaks from the Kevlar fabric substrate.

two parallel NaCl plates. Formation of crystalline ReB_2 of high purity is confirmed by powder XRD (Figure 5G).

Collateral thermal damage of the Kevlar fabric is not evident. SEM images at three different magnifications confirm ReB_2 platelet growth at high platelet number density covering the surfaces of individual Kevlar microfibers (Figure 5B–D). ReB_2 platelets form by an apparent surface-nucleated process giving edge-on attachment in which the ReB_2 (0001) facets are oriented roughly orthogonal to the Kevlar fiber long axis. An oriented-crystal growth process might be expected, as the a -axis of Kevlar (7.87 \AA)⁴¹ and the c -axis of ReB_2 (7.47 \AA) differ in length by only 5%. SEM images at two different magnifications reveal ReB_2 /Kevlar fabric interfaces having exceptionally intimate physical contact (Figure 5E,F).

(41) Northolt, M. G. *Eur. Polym. J.* **1974**, *10*, 799.

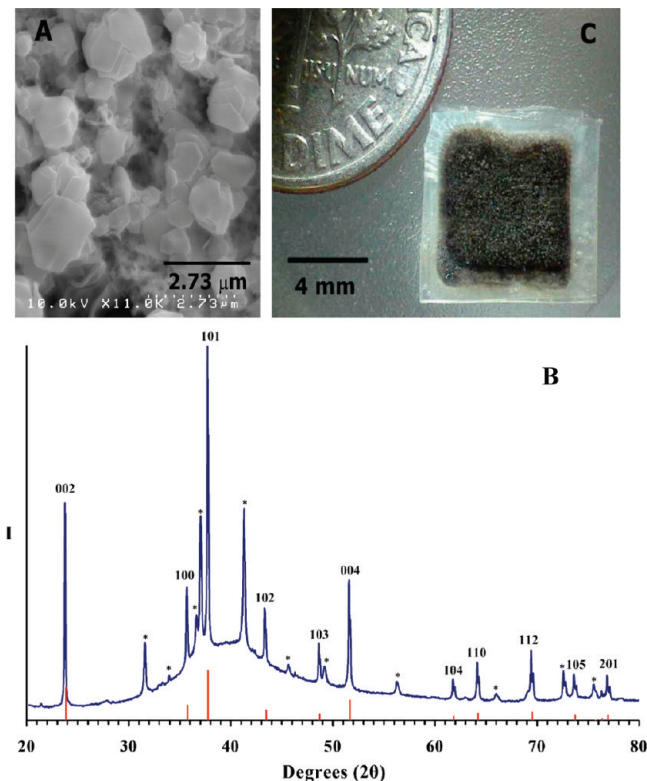


Figure 6. SEM image (A) of ReB_2 hexagonal plates formed on Teflon film. XRD scans (B): ReB_2 particles formed on Teflon substrate (blue); standard XRD line pattern (red) of bulk ReB_2 ; diffraction peaks from the Teflon support denoted as *. Photograph (C) of ReB_2 product formed between two Ultralene films with concomitant shrink-wrapping fusion of the polymer films (partial image of an adjacent U.S. dime coin).

As observed with CPCD processing of precursor **1** on hard supports, irradiation of confined Kevlar fabric specimens wetted with precursor **1** by FEL IR radiation tuned to the B–H stretching band frequency of precursor **1** ($3.9 \mu\text{m}$) also produces a reaction plume and subsequent deposition of a ReB_2 coating. Irradiation of the same specimen with FEL IR light tuned to a frequency off-resonant to any IR absorption band of precursor **1** produces neither a visible reaction plume nor formation of a ReB_2 coating. Irradiation of precursor **1**/Kevlar fabric specimens with FEL IR light tuned to $5.1 \mu\text{m}$ (resonant absorption) supported on *unconfined*, open-faced Si wafer or NaCl plate supports gives visible formation of a reaction plume but only Re metal or Re oxide as crystalline products. Separation of rhenium and boron occurs without intentional spatial confinement of the reaction plume.

Formation of superhard, microcrystalline ReB_2 /Kevlar fabric coatings using CPCD processing has been extended to other partially IR-transmissive polymer supports, such as commercially available IR2 polymer, Teflon, and Ultralene polymer films (Supporting Information). Irradiation of an IR2 plate/precursor **1**/Teflon plate layered assembly with FEL IR light ($5.1 \mu\text{m}$) under ambient atmosphere using the rastering procedure described above forms a black coating of hexagonal microplatelets of ReB_2 (Figure 6A) on both polymer supports, as confirmed by powder XRD (Figure 6B). No obvious collateral thermal damage to either polymer support is evident. Similarly, irradiation of an Ultralene film/precursor **1**/Ultralene film layered sandwich assembly under the same conditions leads to encasement of the expected black product between the two Ultralene polymer films by a “shrink-wrapping” effect (Figure 6C). The

low softening temperature of Ultralene film (120 °C) results in polymer film fusion near the edges of the irradiated area. During the course of this study, XRD data confirmed that ReB_2 particles formed on Si wafers undergo slow air oxidation to form ReO_3 . Air oxidation of metal diboride materials is known and has been studied in detail for ZrB_2 and HfB_2 .³⁷ Being able to prepare metal–boride materials with simultaneous surface-passivation by a shrink-wrapping polymer would be desirable in the formation of ceramics susceptible to oxidation.

Conclusions

Irradiation of single-source or dual-source preceramic precursors confined between hard supports, such as Si wafer or NaCl plates, by resonant, pulsed FEL IR light tuned to precursor carbonyl C=O or B–H stretching band frequencies initiates reaction plume formation and deposition of microcrystalline coatings of ReB_2 , RuB_2 , WB_4 , or B_4C of high purity. Using off-resonant FEL IR irradiation precludes reaction plume formation. Relaxation of spatial precursor confinement leads to element separation. Microcrystalline coatings of known ceramic compositions are produced from this confined-plume, chemical deposition process by rastering the FEL laser beam over a specimen area. Delivery of resonant FEL IR light as a microsecond train of picosecond pulses provides temporal confinement of reaction plume formation, such that crystalline ceramic coatings can be produced on soft supports without causing noticeable thermal damage. Microcrystalline coatings of ReB_2 can be formed directly from a single-source precursor on IR-transmissive IR2, Teflon, or Ultralene polymer films with Ultralene polymer “shrink wrapping” the ReB_2 product during CPCD processing because of its low softening temperature. Exploration of the scope of CPCD as a synthesis strategy for the preparation of other known or postulated hard/superhard materials and more detailed study of the mechanism of ceramic deposition during CPCD processing is anticipated.

Experimental Section

Reagents and General Methods. $\text{Re}(\text{CO})_5\text{Br}$ was either purchased from Strem Chemicals, Inc. or synthesized from $\text{Re}_2(\text{CO})_{10}$ and bromine.⁴² Complex $\text{Re}(\text{CO})_4(\text{B}_3\text{H}_8)$, **1**, was prepared as described in the literature.⁴³ Note: $\text{Re}(\text{CO})_4(\text{B}_3\text{H}_8)$ is moderately air sensitive but can be stored indefinitely as a solid under nitrogen or vacuum in sealed ampules below 0 °C. $\text{Re}_2(\text{CO})_{10}$, $\text{Ru}_3(\text{CO})_{12}$, $\text{W}(\text{CO})_6$, $\text{B}_{10}\text{C}_2\text{H}_{12}$ (*o*-carborane), and $\text{B}_{10}\text{H}_{14}$ (decaborane) were purchased from Strem Chemicals, Inc. $[\text{Me}_4\text{N}][\text{B}_3\text{H}_8]$ was purchased from Dr. Lee J. Todd, Indiana University. All other reagents were purchased from Sigma-Aldrich. Thin-film 3525 Ultralene was purchased from Spex CertiPrep, softened at 120 °C, and pressed into wafers ca. 0.5-mm thick. IR2 polymer was purchased from Fresnel Technologies, Inc. Teflon was purchased from Dupont, and Kevlar was purchased from Fiber Glast Development Corporation. Doped silicon wafers (phosphorus, 1–10 ohms·cm) type N(100) used in microwave experiments were purchased from Silicon, Inc. and were cut to the desired sizes as needed. Undoped, polished silicon fragments with a (510) orientation were purchased from Mr. Dana Smith at The Gem Dugout, Pennsylvania, and cut to the desired sizes as needed. Polished undoped Si(510) wafers were used to prepared samples for easy XRD characterization. Polished and unpolished circular NaCl single-crystal plates 13 mm × 2 mm and 13 mm × 1 mm in size were purchased from International Crystal Laboratories. A commercial FTIR pellet holder (13-mm diameter) was used as the sample holder for FEL laser experiments.

Non-laser-induced thermal treatments were conducted under continuous gas flow inside a quartz tube using a one-foot Linberg/Blue tube furnace or inside a bell-jar chamber within a modified Milestone Drydist microwave reactor (operating at 2.45 GHz). Powder X-ray diffraction scans were obtained on a Scintag $X_1 \theta/\theta$ automated powder X-ray diffractometer with a Cu target, a Peltier-cooled solid-state detector, and a zero-background Si(510) sample support. Powder XRD patterns were analyzed using DICVOL04 to determine space group and approximate unit cell dimensions. Refined unit cell dimensions were calculated using Checkcell to give the following composition, space group, and unit cell parameters [PDF card data] for the microcrystalline materials prepared by CPCD processing: ReB_2 , $P6_3/mmc$, $a = 2.902(1)$ Å, $c = 7.487(4)$ Å [PDF Card #11-0581; $P6_3/mmc$, $a = 2.900$ Å, $c = 7.478$ Å]; RuB_2 , $Pmmn$, $a = 4.628(7)$ Å, $b = 2.860(8)$ Å, $c = 4.046(6)$ Å [PDF Card #15-0213; $Pmmn$, $a = 4.641$ Å, $b = 2.863$ Å, $c = 4.044$ Å]; WB_4 , $P6_3/mmc$, $a = 5.22(3)$, $c = 6.326(2)$ [PDF Card #19-1373; $P6_3/mmc$, $a = 5.200$ Å, $c = 6.340$ Å]; B_4C , $R\bar{3}m$, $a = 5.549(7)$, $c = 12.168(2)$ [PDF Card #35-0798; $R\bar{3}m$, $a = 5.600$ Å, $c = 12.08$ Å].

SEM images were obtained on a Hitachi S-2400 electron microscope with an accelerating voltage at either 5 or 20 kV. Transmission electron microscopic (TEM) bright-field micrographs were recorded on a 200 kV Phillips CM20T TEM.

Confined-Plume Chemical Decomposition Processing Method.

Infrared light produced by the Vanderbilt FEL is tunable from 2 to 9 μm . For a typical experiment intended to synthesize ReB_2 , FEL IR radiation of either 5.1 μm (1960 cm^{-1} ; tuned to the most intense C=O stretching vibration of precursor **1**) or 3.9 μm (2564 cm^{-1} ; tuned to the most intense B–H stretching vibration of precursor **1**) was delivered to samples as 4.0- μs macropulses (30 Hz) where each macropulse of 21.5 mJ energy consists of a series of 0.8- to 1-ps micropulses delivered 350 ps apart. Si wafers (plain or Si(510) wafers) and NaCl wafers were used as sample supports in a sandwich arrangement where precursor (0.05 mL) was placed between two substrates forming a NaCl/precursor **1**/Si wafer assembly. Samples were scanned in a rastering fashion from above the sample through the top NaCl wafer by the FEL IR beam (linear scans (0.5 mm/s) separated spatially by 150 μm). The FEL IR beam was delivered as a spot 350 μm in diameter. FEL experiments were conducted in the open, ambient atmosphere, and samples were stored in sealed glass bell jar flushed with nitrogen.

Single-Source Precursor Synthesis of ReB_2 . $\text{Re}(\text{CO})_4(\text{B}_3\text{H}_8)$ was either deposited (0.05 mL) onto a polished 13 mm × 1 mm NaCl wafer or impregnated on woven Kevlar fabric. The precursor-loaded NaCl or NaCl/Kevlar half assembly was physically pressed together with a Si(510) or clean NaCl wafer forming a completed sandwich assembly and was loaded into a sample holder. FEL irradiation ($\lambda = 5.1$ μm , $E = 21.5$ mJ) was rastered over the sandwich assembly, and then the treated sandwich assembly was characterized by SEM and XRD. ReB_2 film thickness, measured by SEM, for the coated Kevlar fabric specimen is 5–7 μm .

Single-Source Precursor Synthesis of B_4C . *O*-Carborane (0.052 g, 0.091 mmol) was dissolved in benzene (1 mL), and the resulting solution was deposited (0.05 mL) onto a polished 13 mm × 1 mm NaCl wafer and allowed to dry. The precursor-loaded NaCl wafer and a Si(510) wafer were physically pressed together in a sandwich assembly and were loaded into a sample holder. FEL irradiation ($\lambda = 3.85$ μm , $E = 33.0$ mJ) was rastered over the sandwich assembly, and then the treated sandwich assembly was characterized by SEM and XRD. B_4C film thickness, estimated by SEM, for this specimen ranges from 4 to 25 μm .

Dual-Source Precursor Synthesis of WB_4 . $\text{W}(\text{CO})_6$ (0.032 g, 0.091 mmol) and decaborane (0.077 g, 0.630 mmol) were codissolved in tetrahydrofuran (1 mL), and the resulting solution was deposited (0.05 mL) onto a polished 13 mm × 1 mm NaCl wafer and allowed to dry. The precursor-loaded NaCl wafer and a Si(510) wafer were physically pressed together in a sandwich assembly and loaded into a sample holder. FEL irradiation ($\lambda = 5.1$ μm , $E =$

(42) Schmidt, S. P.; Trogler, W. C.; Basolo, F.; Urbancic, M. A.; Shapley, J. R. *Inorg. Synth.* **1990**, 28, 160.

(43) Gaines, D. F.; Hildebrandt, S. J. *Inorg. Chem.* **1978**, 17, 794.

21.5 mJ) was rastered over the sandwich assembly, and then the treated sandwich assembly was characterized by SEM and XRD. WB_4 film thickness, estimated by SEM, for this specimen ranges from 0.6 to 2 μm .

Dual-Source Precursor Synthesis of RuB_2 . $\text{Ru}_3(\text{CO})_{12}$ (0.006 g, 0.009 mmol) and decaborane (0.024 g, 0.196 mmol) were codissolved in tetrahydrofuran (1 mL), and the resulting solution was deposited (0.05 mL) onto a polished 13 mm \times 1 mm NaCl wafer and allowed to dry. The precursor-loaded NaCl wafer and a Si(510) wafer were physically pressed together in a sandwich assembly and loaded into the sample holder. FEL irradiation ($\lambda = 5.1 \mu\text{m}$, $E = 21.5 \text{ mJ}$) was rastered over the sandwich assembly, and then the treated sandwich assembly was characterized by SEM and XRD. RuB_2 film thickness, estimated by SEM, for this specimen ranges from 4 to 30 μm .

Dual-Source Precursor Synthesis of ReB_2 . $\text{Re}_2(\text{CO})_{10}$ (0.020 g, 0.031 mmol) and decaborane (0.055 g, 0.450 mmol) were codissolved in tetrahydrofuran (1 mL), and the resulting solution was deposited (0.05 mL) onto a polished 13 mm \times 1 mm NaCl wafer and allowed to dry. The precursor-loaded NaCl wafer and a Si(510) wafer were physically pressed together in a sandwich assembly and loaded into a sample holder. FEL irradiation ($\lambda = 5.1 \mu\text{m}$, $E = 30.0 \text{ mJ}$) was rastered over the sandwich assembly, and then the treated sandwich assembly was characterized by SEM and XRD (Supporting Information). ReB_2 film thickness, estimated by SEM, for this specimen ranges from 0.6 to 3 μm .

Non-Laser-Induced Synthetic Attempts To Prepare ReB_2 . The importance of using resonant FEL IR light to degrade precursors was investigated via control experiments with $\text{Re}(\text{CO})_4(\text{B}_3\text{H}_8)$. Si wafer/ $\text{Re}(\text{CO})_4(\text{B}_3\text{H}_8)$ /Si wafer samples were assembled, placed into a quartz boat, and heated in a tube furnace under a N_2 atmosphere at 700 $^\circ\text{C}$ for 2 h. Both of the inside surfaces of the Si wafer/Si wafer interface were coated with a silvery residue determined to be Re metal by XRD. No detectable formation of ReB_2 was observed. A Si wafer/ $\text{Re}(\text{CO})_4(\text{B}_3\text{H}_8)$ /Si wafer sample was heated rapidly to high temperature using a novel microwave process.⁴⁴ The sample specimen was placed inside an enclosed glass bell jar

within a microwave reactor cavity. The bell jar was purged with argon gas, irradiated with microwave radiation (300 W, 10 min, $T > 400 \text{ }^\circ\text{C}$), and allowed to cool to room temperature. Separation of the silicon wafers revealed an amorphous red decomposition product that exhibited no identifiable crystalline peaks by powder XRD. When this sample was heated in a tube furnace under a N_2 atmosphere at 700 $^\circ\text{C}$ for 2 h, a silver residue of Re metal (as determined by XRD) formed at the Si wafer/Si wafer interface. Neither conventional nor microwave heating of Si wafer/ $\text{Re}(\text{CO})_4(\text{B}_3\text{H}_8)$ /Si wafer sample specimens to elevated temperatures gave detectable formation of ReB_2 .

Off-Resonant CPCD Synthesis Attempts To Prepare ReB_2 . The importance of using resonant FEL IR light to degrade precursors was investigated via control experiments by attempting to prepare ReB_2 from $\text{Re}(\text{CO})_4(\text{B}_3\text{H}_8)$ using nonresonant FEL IR laser energy. Two FEL IR nonresonant experiments were conducted on NaCl/ $\text{Re}(\text{CO})_4(\text{B}_3\text{H}_8)$ /NaCl wafer assemblies. FEL irradiation ($\lambda = 4.5 \mu\text{m}$, $E = 4.5 \text{ mJ}$) was rastered over the sandwich assembly during which no illuminated plume was visible. The wafer assemblies were separated, visual inspection demonstrated no solids, and subsequent XRD scans were void of any crystalline material.

Acknowledgment. We thank Dr. David W. Piston for access to the Vanderbilt University Free-Electron Laser Facility, Dr. John Kozub and all FEL staff for vigorous and qualified support and for use of borrowed equipment during experiments, and Vanderbilt University for support of this research.

Supporting Information Available: Cartoon depicting the CPCD synthesis procedure, powder XRD scan of ReB_2 synthesized from dual source precursors, pressure and temperature estimation of the *o*-carborane ($\text{B}_{10}\text{C}_2\text{H}_{12}$) decomposition plume, infrared absorption spectral data for selected precursors and confinement support materials. This material is available free of charge via the Internet at <http://pubs.acs.org>.

(44) Boxall, D. L.; Lukehart, C. M. *Chem. Mater.* **2001**, *13*, 806.